AN EXPERIMENTAL AND THEORETICAL INVESTIGATION ON THE INTRAMOLECULAR CHARGE TRANSFER PROPERTIES OF p-DIMETHYLAMINOBENZALDEHYDE

Abstract

Excited state charge transfer (CT) reaction is not so common for a molecule containing a weak donor and a weak acceptor group. For example, p-dimethylaminobenzaldehyde (DMABA), where –CHO is a weak charge acceptor and $–NMe_2$ is a weak donor. In spite of several studies, the charge transfer ability of DMABA still remains unclear and deserves further attention. In this chapter, the excited state CT properties of DMABA are explored through experimental as well as computational studies. While experimental absorption and fluorescence spectra are recorded and reported, quantum chemical methods are adopted to obtain the theoretical results. Density Functional Theory (DFT) with B3LYP functional and 6-311++G** basis set is used to compute the potential energy surfaces along the twisting angles of both donor and acceptor groups. Also investigated is the solvent effect on the emission spectra of DMABA by Time Dependent Density Functional Theory Polarization Continuum (TDDFT-PCM) model.

Keywords: Twisted intramolecular charge transfer, p-dimethylaminobenzaldehyde, Density Functional Theory, Potential energy surface

Author

Dr. Anuva Samanta
Assistant Professor
Department of Chemistry
Victoria Institution (College)
Kolkata, West Bengal, India
anuva.samanta25@gmail.com

I. INTRODUCTION AND OBJECTIVES

Due to its dual emission behavior, 4-(N,N-dimethylamino)benzonitrile (DMABN) has received enormous attention in the literature from both theoretical as well as experimental approaches. However, to a surprise, enough information is not available for its precursor molecule, namely, p-dimethylaminobenzaldehyde (DMABA). Thus, DMABA and its photophysical properties are of the particular interest of this work. It may be important to note here that moving from DMABN to DMABA, a strong acceptor group -CN is replaced a comparatively weaker acceptor -CHO group. It has already been reported that DMABA also shows dual fluorescence emission in polar solvent, which could be due to the formation of a conformation of intramolecular charge transfer (ICT) [1-5]. The local emission (LE) peak of DMABA in different solvents with different polarity appeared in the range of 370 – 390 nm [2], while the CT emission was reported around 490 – 510 nm [2], except for acetonitrile (ACN) and N, N-dimethyl formamide (DMF) solvents. The CT emission peak for these two solvents is at ~600 nm [2,6] and could not be reproduced in the current work. In the present work, the low energy emission peak of DMABA is observed at ~550 nm. However, to confirm the current experimental findings the photophysical properties of DMABA are reinvestigated for a variety of solvents with different polarity. In addition, a detailed theoretical investigation has also been performed for DMABA to correspond the experimental findings. To the best of our knowledge, the detailed theoretical results in terms of the potential energy surface is missing in the literature and thus, thus the current investigation would be an important contribution to the related community. Density functional theory with Becke, 3-parameter, Lee–Yang–Parr (B3LYP) functional [7] is implemented to find the minimum energy geometry of the molecule as well as the potential energy surface at ground and excited state in vacuum and in acetonitrile solvent. The solvent effect is taken under Polarization Continuum Model (PCM) approximation. 6-311++G** basis set is used for all these calculations. Also investigated are the potential energy surfaces by independent rotation of the donor $–NMe_2$ group as well as acceptor –CHO group for both the ground and excited states. The potential energy scan shows a second minimum of DMABA at S_1 state at a twist angle of 90^0 of either rotation. Such a result reinforces the proposed Twisted Intramolecular Charge Transfer (TICT) model that exists in DMABA.

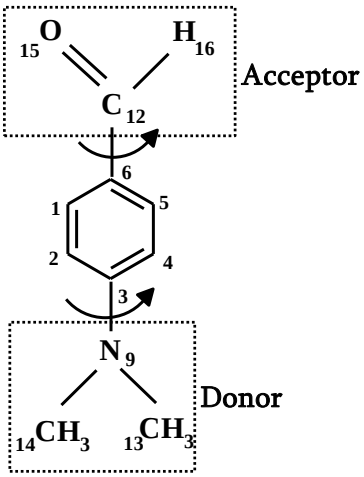

Scheme 1: Structure of p-dimethylaminobenzaldehyde (DMABA).

II. EXPERIMENTAL DETAILS

Reagents: The molecule DMABA (Scheme 1) was purchased from Sigma-Aldrich and no further purification was done. For the preparation of different solutions, spectroscopic grade solvents are used.

III. INSTRUMENTATION AND METHODS

All the steady state absorption spectral measurements were performed by Hitachi UV/VIS (Model U-3501) spectrophotometer using a quartz cuvette of 1cm optical path length. The steady state fluorescence spectra were recorded by using PerkinElmer (Model LS-55) fluorimeter [8].

IV. COMPUTATIONAL DETAILS

For the theoretical electronic structure calculations, Hartree-Fock (HF) and Density Functional Theory (DFT) are implemented to obtain the minimum energy geometries of all the molecule. The structural optimization of DMABA in the presence of solvents is computed using Polarized Continuum Model (PCM) [9-11]. To understand the ICT phenomena of DMABA, potential energy surfaces (PES) are calculated for the ground (S_0) state as well as two excited states, namely S_1 and S_2. Time dependent DFT (TDDFT) method is adopted for all the excited state calculations, whereas TDDFT-PCM method is followed for obtaining the solvent effect on the excited state. The PES are scanned over a twist angle of $–NMe_2$ group as well as –CHO group from -20 to 120° separately. The calculations of PESs are the following: One of the functional groups is rotated from -20 to 120° with an increment of 10° at a time. B3LYP/6-311++G** level of theory is used to calculate the potential energy surface at S_0 state. For this scan, all other structural parameters are kept frozen. Once the surface is obtained at S_0 state, the vertical excitation energy corresponding to each of the S_0 geometries is calculated using TDDFT method to generate the PES at S_1 state. All the calculations are performed in Gaussian03 software [12]. It is worth to mention here that the TDDFT method has a few limitations, namely, it cannot predict correct vertical excitation energy for the (1) excitation to the Rydberg state [13], (2) excitation of the dissociating molecules [14], and (3) long-range charge transfer excitations for larger molecules [15]. In addition, geometry optimization at the excited states could not be performed using TDDFT method. Nevertheless, the results obtained from this method of theory correspond well with the experimental counterpart [9-11].

V. RESULTS AND DISCUSSION

Absorption Study: The absorption spectra of DMABA are examined for a variety of solvents from low to high polarity. DMABA exhibits a strong absorption band at ~340 nm and a weak band at ~300 nm, which are known to be for ground state to L_a and L_b state transitions, respectively. The absorption spectra of DMABA for all solvent systems are depicted in figure 1. The low energy absorption band is associated with a large molar extinction coefficient and is for the π to π^* transition of the benzene moiety. A profound solvent effect is found to exist for the higher wavelength (low energy) absorption band, whereas the high energy band remains unaffected with solvent polarity. In general, for normal donor-acceptor molecules, the absorption band was seen to be blue shifted in presence

of a polar protic solvent [16-19]. This may be due to the formation of Hydrogen-bonded cluster in those solvents. On the contrary, the present molecule, DMABA is seen to be red shifted in presence of polar protic solvent. With changing polarity of the solvents from non-polar to polar protic, DMABA shows a consistent red shift of the absorption band [2,5]. When water is used, the absorption maxima are located at ~353 nm. It may be noted that the DMABA is capable of forming H-bond in both the donor and acceptor sites. At the donor site, the lone pair of Nitrogen can be used, whereas the aldehyde group at the acceptor site is a potential candidate for H-bond formation. However, the Mulliken charge at the Nitrogen atom is more negative than the Oxygen atom. Th unusual blue shift of the absorption band of DMABA is because of the fact that the dielectric property dominates over H-bonding ability of water. In Table 1 the spectral properties of DMABA in presence of all the solvents are summarized.

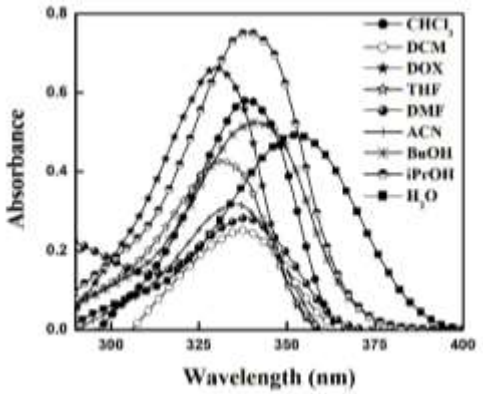

Figure 1: UV-vis absorption spectra of DMABA. The spectra are obtained at room temperature and in different solvents

Table 1: Spectroscopic parameters of DMABA molecule at room temperature measured by absorption and fluorescence spectroscopic techniques.

Solvents	λ_{Abs} **(nm)**	λ_{Em} **(nm)**	$\Delta\bar{\nu}$ **(cm^{-1})**
DOX	330	379, 458	4869
$CHCl_3$	339	382, 470	8222
DCM	338	381, 492	9260
THF	332	382, 480	9287
ACN	336	389, 556	11776
DMF	338	385, 552	11470
MeOH	340	410	5021
H_2O	353	420	4519

VI. FLUORESCENCE STUDY

Like absorption analyses, the emission spectra of DMABA are also investigated in all the solvents and the results are shown in Figure 2a. The maxima positions of the fluorescence bands are tabulated in Table 1. DMABA does not show any detectable fluorescence in non-polar hydrocarbon solution. In polar solvents, DMABA shows dual fluorescence bands upon 340 nm excitation. One at 385 nm which is assigned as local emission (LE) and another at ~520 nm. The higher wavelength band is known from the literature as for the intramolecular charge transfer state (ICT) [2-5]. With the change in solvent polarity, the position of the LE and Charge Transfer (CT) bands in the fluorescence spectra is seen to change. But the one for the ICT state is seen to change significantly. The position of the ICT state is shifted towards higher wavelengths for the solvent with higher dielectric constant. In a couple of previous studies [1,2], the CT band of DMABA is reported at ~600 nm in DMF [1] and ACN [2] solvents. However, in the present study, as reported in Figure 2a, the emission spectra have a maximum at ~550 nm. This result is similar to the one reported in an earlier article [10], which reported the CT emission band at ~550 nm. In Figure 2b, the excitation spectra tracked at various λ_{max} values of that of the absorption spectra of DMABA are shown. The two fluorescence bands as appeared for the CAN solvent do not differ much with the excitation wavelengths. Hence, the bands are assigned to the ground state absorbing at ~340 nm. In hydroxylic solvents, namely, BuOH, iPrOH, etc., the dual emission of DMABA is also observed. Conversely if the H-bond ability of the solvent increases, single emission band of DMABA is observed. This could be due to lowering of the energy gap between the Franck-Condon state and the ICT state, which results in a rapid non-radiative decay to the ground state or maybe to a low-lying triplet states [20]. In Figure 2c, the emission spectra in a binary mixture of the solvent are shown. In this study ACN is mixed with MeOH with different percentages. When the concentration of methanol is increased, the intensity of both the bands decreases. This result also proves that with increasing polarity and H-bonding ability, the chances of non-radiative decay channels enhance. Therefore, the rate of intersystem crossing increases at the expense of fluorescence intensity.

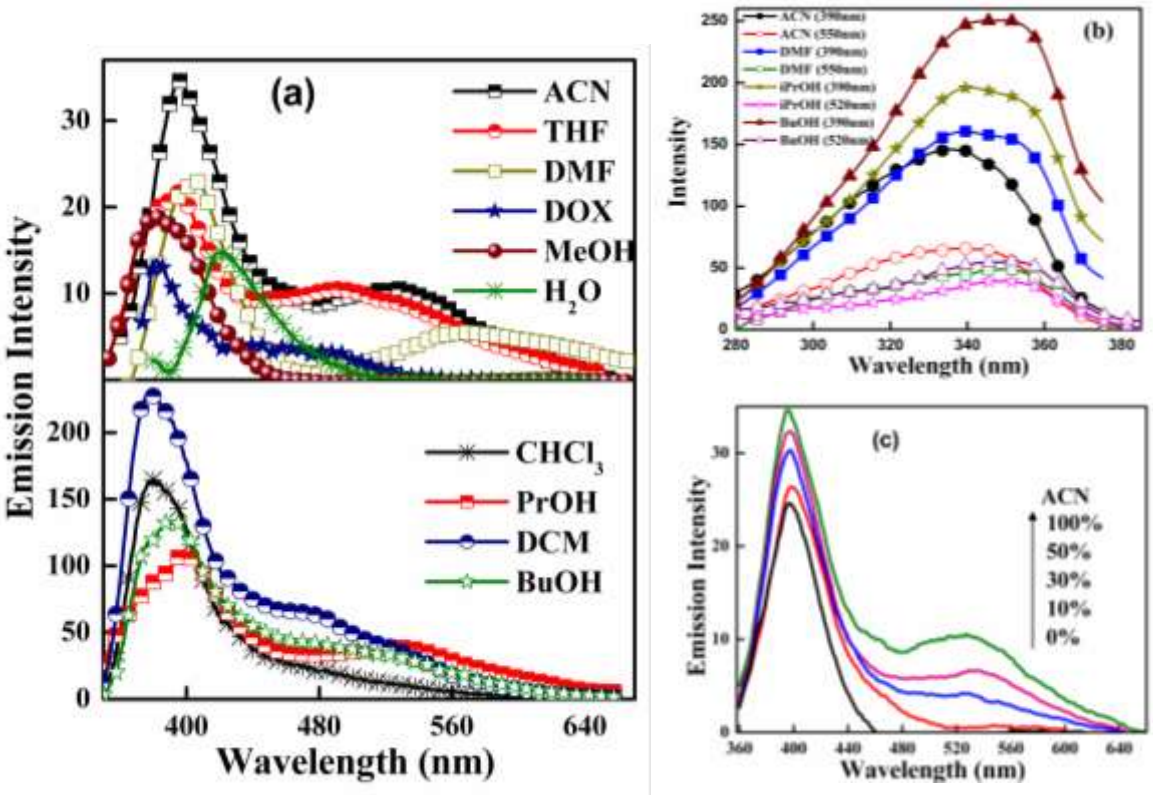

Figure 2: (a) Fluorescence emission spectra of DMABA (Steady State) at room temperature and in different solvents. (b) Fluorescence excitation spectra at room temperature and in different solvents. (c) Effect of binary solvent mixture (ACN+MeOH) on the emission spectra (λ_{ext}=340nm).

VII. THEORETICAL CALCULATIONS

The experimental evidence of the dual fluorescence behavior of DMABA emphasizing the ICT model is validated through theoretical electronic structure calculation using Density Functional Theory (DFT). The minimum energy geometry of DMABA in the ground S_0 state, and potential energy surface (PES) for both ground and excited states are calculated at B3LYP/6-322++G** level of theory. Also computed at the same lever is the Mulliken charge distribution of optimized DMABA. In Table 2, all the structural information is listed.

Table 2: Structural parameters of DMABA in the ground state as obtained from B3LYP/6-311++G level.**

Bonds	Values (Å)	Angle/Dihedral	Values (°)
C1-C2	1.38	∠C13-N9-C14	119.3
C2-C3	1.42	∠C13-N9-C3	120.2
C3-C4	1.42	∠C1-C6-O12	120.3
C6-C1	1.40	∠C2-C3-N9-C13	0.04
C6-C12	1.47		

C12-O15	1.22		
C3-N9	1.37		
N9-C13	1.45		
N9-C14	1.46		

In the global minimum geometry, DMABA exists in a nearly planner configuration with $–NMe_2$ group in the plane of the benzene ring and the calculated angle $\angle C_2\text{-}C_3\text{-}N_9\text{-}C_{13}$=0.04, i.e., very close to zero. Therefore, the lone pair of N-atom is expected to take part in the conjugation with the benzene ring. It is already well known from the literature [16-19] that for ICT model, a twisted geometry (either in terms of $–NMe_2$ group or –CHO group, in the present study) in the ground state favors the ICT reaction in the excited state. Thus, the global minimum geometry of DMABA does not support the excited state ICT reaction at all. The potential energy at S_0 and S_1 states are scanned as a function of the rotation angle of both $–NMe_2$ and –CHO group, which is varied from -20° to 120° with 10° increment at each step. In this scan, no geometry optimization at different electronic states is performed. For the ground state calculation DFT method is implemented for the vacuum calculation and DFT-PCM model is used to examine the solvent (ACN) effects. For excited state calculations, the corresponding methods that are adopted are TDDFT and TDDFT-PCM. In Figure 3 the potential energy scan with the variation of the rotation angle of the donor dimethylamino group is presented.

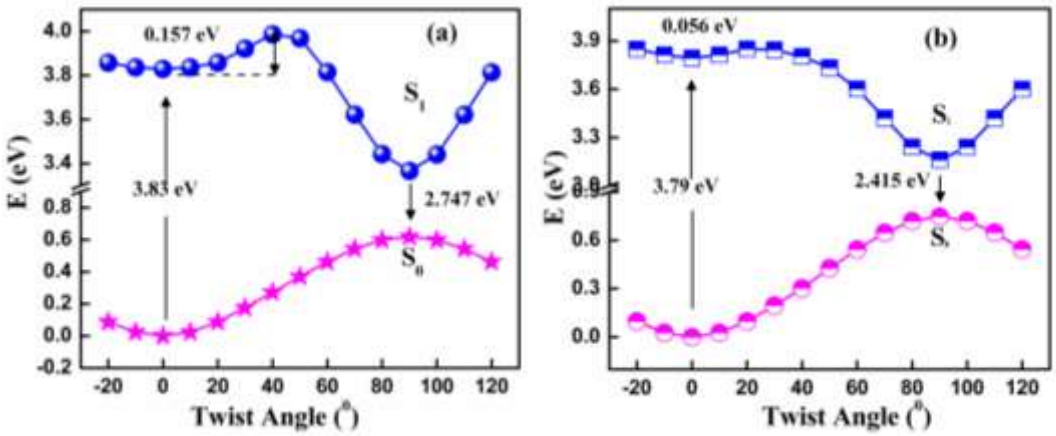

Figure 3: Potential energy scan as a function of donor rotation angle ($\angle C_2\text{-}C_3\text{-}N_9\text{-}C_{13}$) of DMABA for S_0 and S_1 states in (a) vacuum and (b) ACN solvent at B3LYP/6-311++G** level

PES scan shows that at S_0 state a minimum is located at untwisted geometry (i.e., θ = 0°) and a maximum at θ = 90°. The rotation barrier at S_0 state is about 0.62 eV. On the other hand, at S_1 state, DMABA exhibits two minima at θ = 0° and θ = 90°, respectively. The transition at θ = 0° is associated with local emission, whereas the one at θ = 90° is regarded as CT emission. The barrier height from the local state to the CT state at the S_1 potential energy surface is lower than that of S_0 surface and is discussed below. When the same scan is performed for the ACN solvent using TDDFT-PCM model, the barrier for the local to CT state transition at the S_1 surface becomes even lower and the twisted geometry is more stabilized in ACN. Since the minimum energy geometry of DMABA in the ground state is

non-twisted, the absorption is expected to take place from this geometry. The computed vertical excitation energies of 3.83eV and 3.79eV, respectively in gas phase and in ACN solvent are in excellent agreement with the corresponding experimental values of 3.85eV in MCH and 3.70eV in ACN solvent (see Table 3). The vertical excitation energy decreases while moving from vacuum to ACN solvent. This explains the red-shift behavior of the normal fluorescence band with increasing polarity. Also calculated are the vertical excitation energies from S_0 to S_2 state in vacuum as well as in ACN. The calculated values of 4.15 eV (vacuum) and 3.96 eV (ACN) are again in excellent agreement with experimental value of 4.13 eV for both the cases.

Table 3: Vertical excitation energies (eV) of DMABA in vacuum and ACN solvent calculated at B3LYP/6-311++G level, and comparison with the corresponding experimental values.**

Medium/Solvent	Absorption (eV)			Emission (eV)		
	State	E_{th}	E_{ex}	State	E_{th}[a]	E_{ex}[a]
Vacuum	S_1	3.83	3.85[b]	S_1	2.75	-
	S_2	4.15	4.13[b]	S_2	-	-
ACN	S_1	3.79	3.70	S_1	2.42	2.25
	S_2	3.96	4.13	S_2	-	-

[a]Emission from CT state. E_{th} and E_{ex} are theoretical and experimental energy, respectively. [b]Absorption taken in MCH solvent.

As mentioned above, the emission from the non-twisted geometry ($\theta = 0^0$) is regarded as the LE emission, whereas the one from the twisted geometry ($\theta = 90^0$) is Twisted ICT emission. From the computed PESs it is found that the barrier for the transition from LE to the TICT state decreases from 0.157eV (vacuum) to 0.056eV (ACN) at S_1 surface. This decreasing of the barrier height in the excited state in ACN solvent is the reason of TICT formation in the S_1 state. Similar to the rotation of $-NMe_2$ case, the twisting of the acceptor group ($\angle C_5$-C_6-C_{12}-O_{15}) also generates a single well in the ground state with a minimum at $\theta = 0°$, whereas double minimum in the S_1 state at $\theta = 0°$ and $\theta = 90°$, respectively (see Figure 4). However, in this case, the barrier height from LE to TICT state at S_1 surface is more than that obtained for $-NMe_2$ rotation.

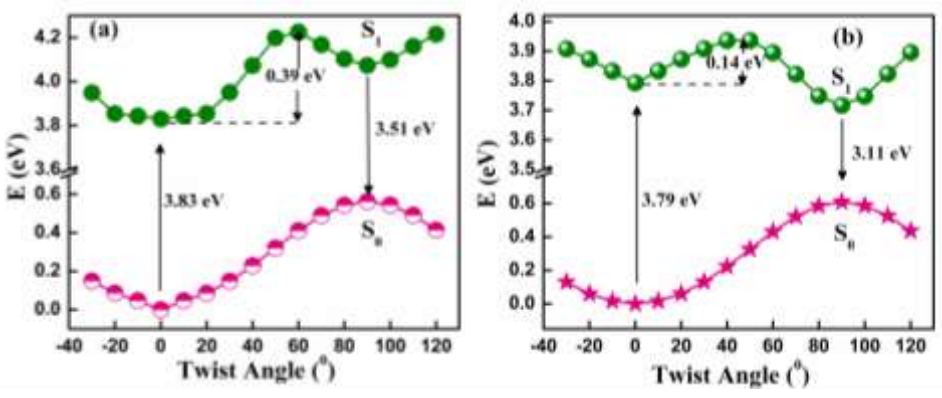

Figure 4: Same as Figure 3, but for the twist angle ($\angle C_5$-C_6-C_{12}-O_{15}) of DMABA

Thus, the twisting of acceptor group is less favorable than that of donor group. The barrier height energies from LE state to TICN state are 0.39eV in vacuum and 0.14eV in CAN, whereas the twisting path of $–NMe_2$ group shows a shift to longer wavelength (lower energy/red shift) for the emission from the TICT state. In Figure 5, the change in vertical excitation energy and oscillator strength for the S_1 state are shown for vacuum and ACN solvent. As one can see the $\pi \rightarrow \pi^*$ transition is an allowed transition and is associated with very high oscillator strength (0.63). This transition is for the untwisted structure, i.e., $\theta = 0°$, whereas the CT emission at $\theta = 90°$ is the $n \rightarrow \pi^*$ transition and the corresponding oscillator strength is very low (0.00). This observation is opposite to the one reported previously for other donor-acceptor systems [16-19]. It was seen for those molecules that the CT state shows higher emission intensity than the LE state. However, for the present study of DMABA, the theoretical findings are in good agreement with the experimental ones.

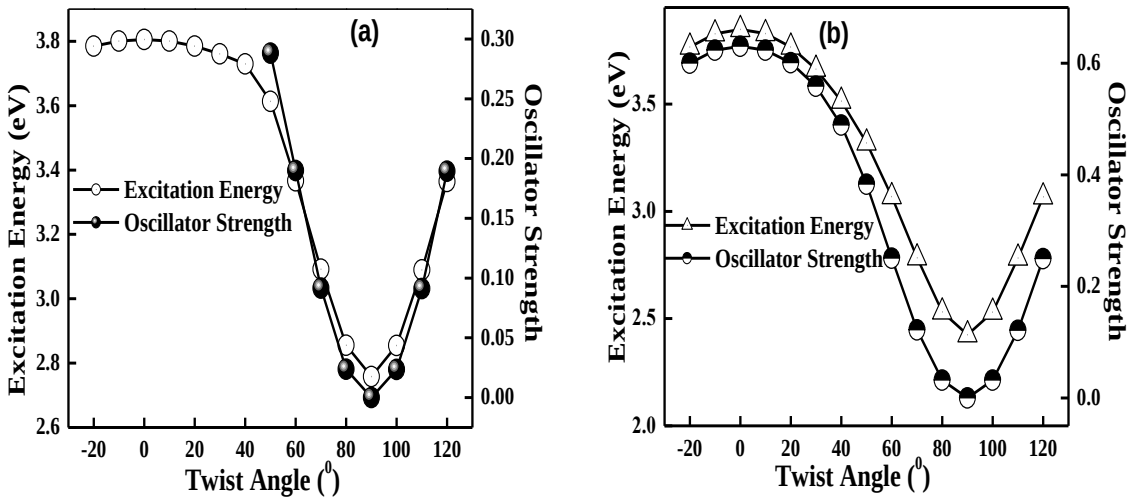

Figure 5: The change of vertical excitation energies and oscillator strength with varying donor twist coordinate in (a) vacuum and (b) ACN.

The frontier molecular orbital picture as shown in Figure 6 also explains the current TICT model in the excited state. In the case of untwisted geometry, i.e., $\theta = 0°$, the π-electron density is delocalized across the aromatic ring for both the HOMO (π) and LUMO (π^*) MOs. Therefore, the LE emission is of $\pi \rightarrow \pi^*$ transition. On the other hand, when the twisted geometry, i.e., $\theta = 90°$, is considered, π-electron density is localized on the N-atom of $–NMe_2$ group. Thus, this HOMO (n) and LUMO (π^*) are responsible for the $n \rightarrow \pi^*$ transition showing CT emission. Therefore, one can conclude that the localized nitrogen lone pair at the 90^0 twisted geometry is responsible for the CT emission.

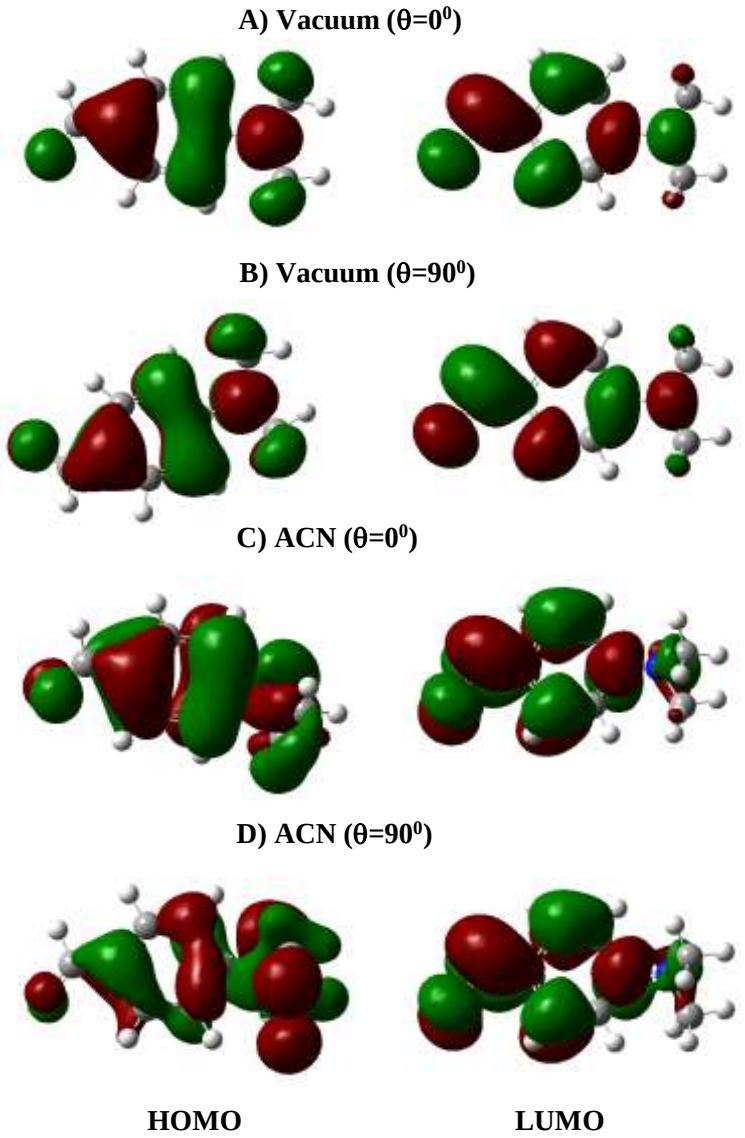

Figure 6: Frontier molecular orbital pictures of HOMO and LUMO of DMABA for the twist angle θ = 0°: (A) vacuum and (B) ACN solvent, and for the twist angle θ = 90°: (C) vacuum and (D) ACN solvent.

VIII. CONCLUSION

The photophysical properties, particularly the dual emission behavior of DMABA, are investigated using spectroscopic techniques supported by electronic structure calculation implementing density functional theory. The dual emission of DMABA is due to the local emission and the charge transfer emission from the excited state, where the local emission associated with normal Stokes shifts. The presently observed position of the CT band in DMF and ACN solvents is different from the ones reported by Grabowski et al. [1] and Kawski et al. [2]. The global minimum geometry of DMABA is obtained, which shows that the $–NMe_2$ group is in the same plane of the aromatic ring. The potential energy surfaces at both S_0 and S_1 state are computed by varying the rotation (twist) angle of $–NMe_2$ as well as –CHO group,

separately, where TDDFT method is used for the calculation in S_1 state. The calculated S_1 surface shows a double well potential, where the positions of the minima are located at the twist angle of 0° and 90°. This validates a LE→TICT state transition. The theoretical calculations also suggest that the donor ($–NMe_2$) twist motion is preferred over the one for the acceptor (–CHO) as the latter proceeded with a higher barrier height. TDDFT-PCM method is then implemented to calculate the PESs in presence of ACN solvent. It was observed that in presence of polar solvent the height of the LE → TICT transition barrier further reduces enhancing the chance of ICT emission. The computed oscillator strength for the emission suggests that the molecules provide a stronger local emission and a weak charge transfer emission. Frontier molecular orbital pictures proves that for LE a of $\pi \rightarrow \pi^*$ transition is taking place whereas for ICT, an $n \rightarrow \pi^*$ transition occurs as a localized lone pair electron density on N-atom is seen for the twist angle of 90°.

REFERENCES

[1] Z. Grabowski and J. Dobkowski, *Pure Appl. Chem.*, 1983, 55, 245
[2] A. Kawski, B. Kukliński and P. Bojarski, *Chem. Phys. Lett.*, 2007, 448, 208.
[3] S. Dähne, W. Freyer, K. Teuchner, J. Dobkowski and Z. R. Grabowski, *J. Lumin.*, 1980, 22, 37.
[4] N. Chattopadhyay, J. Rommens, M. V. Auweraer and F. C. D. Schryver, *Chem. Phys. Lett.*, 1997, 264, 265.
[5] A. Kawski, B. Kukliński and P. Bojarski, *Chem. Phys. Lett.*, 2008, 455, 52.
[6] Z. Grabowski, K. Rotkiewicz and W. Rettig, *Chem. Rev.*, 2003, 103, 3899.
[7] C. Lee, W. Yang and R. G. Parr, *Phys. Rev. B*,1988, 37, 785.
[8] J.R. Lakowicz, Principles of Fluorescence Spectroscopy, Springer, 3rd edition, 2006.
[9] A. Samanta, B. K. Paul, S. Mahanta, R. B. Singh, S. Kar and N. Guchhait, *J. Photochem. Photobiol. A: Chem.*, 2010, 212, 161.
[10] A. Samanta, B. K. Paul and N. Guchhait, *J. Lumin.*, 2012, 132, 517.
[11] B. K. Paul, A. Samanta, S. Kar and N. Guchhait, *J. Lumin.* 2010, 130, 1258.
[12] Gaussian 03, Revision B.03, M. J. Frisch *et al.* Gaussian, Inc., Pittsburgh PA, 2003.[13] C. Adamo, G.
[13] E. Scuseria, and V. Barone, J. Chem. Phys. 111 (1999) 2889-2899.
[14] Z. L. Cai, and J. R. Reimers, *J. Chem. Phys.*, 2000, 112, 527.
[15] J. Neugebauer, O. Gritsebko and E. Jan Baerends, *J. Chem. Phys.*, 2006, 124, 214102.
[16] R. B. Singh, S. Mahanta, S. Kar and N. Guchhait, *Chem. Phys.*, 2007, 342, 33.
[17] S. Mahanta, R. B. Singh, S. Kar and N. Guchhait, *J. Photochem. Photobiol. A: Chem.*, 2008, 194, 318.
[18] A. Chakraborty, S. Kar and N. Guchhait, *J. Photochem. Photobiol. A: Chem.*, 2006, 181, 246.
[19] S. Kundu and N. Chattopadhyay, *J. Photochem. Photobiol. A: Chem.*, 1995, 88, 105.

